



## RESEARCH ARTICLE

# Deciphering binding mechanism between bovine serum albumin and new pyrazoline compound K4

Ebru Bozkurt<sup>1</sup> | Halise Inci Gul<sup>2</sup>

<sup>1</sup>Programme of Occupational Health and Safety, Erzurum Vocational Training School, Ataturk University, Erzurum, Turkey

<sup>2</sup>Department of Pharmaceutical Chemistry, Faculty of Pharmacy, Ataturk University, Erzurum, Turkey

**Correspondence**

Ebru Bozkurt, Program of Occupational Health and Safety, Erzurum Vocational Training School, Ataturk University, 25240 Erzurum, Turkey.

Email: ebrubozkurt@atauni.edu.tr

**Abstract**

The binding mechanism of a new and possible drug candidate pyrazoline derivative compound **K4** and bovine serum albumin (BSA) was investigated in buffer solution (pH 7.4) using ultraviolet–visible light absorption and steady-state and synchronous fluorescence techniques. The fluorescence intensity of BSA was quenched in the presence of **K4**. The quenching process between BSA and **K4** was examined at four different temperatures. Decrease of the quenching constants calculated using the Stern–Volmer equation and at increasing temperature suggested that the interaction BSA–**K4** was realized through a static quenching mechanism. Synchronous fluorescence measurements suggested that **K4** bounded to BSA at the tryptophan region. Fourier transform infrared spectroscopy results showed that there was no significant change in polarity around the tryptophan residue. The forces responsible for the BSA–**K4** interaction were examined using thermodynamic parameters. In this study, the calculated negative value of  $\Delta G$ , the negative value of  $\Delta H$  and the positive value of  $\Delta S$  pointed to the interaction being through spontaneous and electrostatic interactions that were dominant for our cases. This study provides a very useful *in vitro* model to researchers by mimicking *in vivo* conditions to estimate interactions between a possible drug candidate or a drug and body proteins.

**KEYWORDS**

bovine serum albumin, fluorescence quenching, FRET, pyrazoline

## 1 | INTRODUCTION

Studies on the interaction between proteins and fluorescent probes are very important as they act as models for biochemical applications in cells.<sup>[1–3]</sup> Serum albumins are proteins that constitute approximately 60% of total plasma proteins. These proteins play an important role in the transport of exogenous and endogenous substances such as fatty acids, metal ions, drugs, and dyes. Bovine serum albumin (BSA) and human serum albumin (HSA) are proteins that are frequently used in biochemical and biophysical studies. BSA is the 76% structural homologue of HSA. BSA is generally preferred as a model protein due to its ease of use, low cost, stability, and unusual ligand binding properties in laboratory experiments.<sup>[4]</sup> Spectroscopic techniques such as ultraviolet–visible (UV–vis) light absorption, and

steady-state and time-resolved fluorescence measurements are often used to investigate the interactions between BSA or HSA and fluorescence probes due to their ease of use, accuracy, high precision, and rapid response.<sup>[5–7]</sup>

Pyrazoline derivatives are compounds with antimicrobial,<sup>[8]</sup> antinociceptive,<sup>[9]</sup> anticancer,<sup>[10,11]</sup> antidepressant,<sup>[12]</sup> and anti-inflammatory<sup>[13]</sup> properties. In addition to the pharmacological importance of these compounds, they are used as fluorescent compounds because of their strong fluorescence properties and high quantum yields. To understand the interaction of these bioactive fluorescent compounds with protein molecules in the cell, studies in the laboratory environment with model systems constitute a marked research area.<sup>[14,15]</sup> Therefore, it is very important to understand the interaction mechanisms between new pyrazoline derivatives and BSA.

This study aimed to investigate the binding mechanism between BSA and a new pyrazoline derivative 4-(3-(3,4,5-trimethoxyphenyl)-3a,4-dihydroindeno[1,2-c]pyrazol-2(3H)-yl)benzenesulfonamide (**K4**) (Scheme 1) in Tris-HCl buffer solution (pH 7.4) using UV-vis light absorption, and steady-state and synchronous fluorescence measurements. **K4** was selected from a series of synthesized compounds described in our previous study<sup>[16]</sup> because of its interesting cytotoxic activity. Binding mechanism parameters such as binding constant, binding mode, binding site, and binding distance between BSA and **K4** were determined and will provide extra information on how the conformation and structure of BSA changes due to the binding to **K4**. The results obtained from the presented study will explain the binding mechanism between the possible drug candidate compound **K4** and BSA. Compound **K4** and BSA constitute a model system that were realized *in vitro* but mimic *in vivo* physiological conditions. This model describes a very useful and practical approach to estimate the interaction between a compound (**K4**), a possible drug candidate, and body proteins.

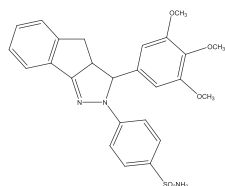
## 2 | EXPERIMENTAL

### 2.1 | Materials

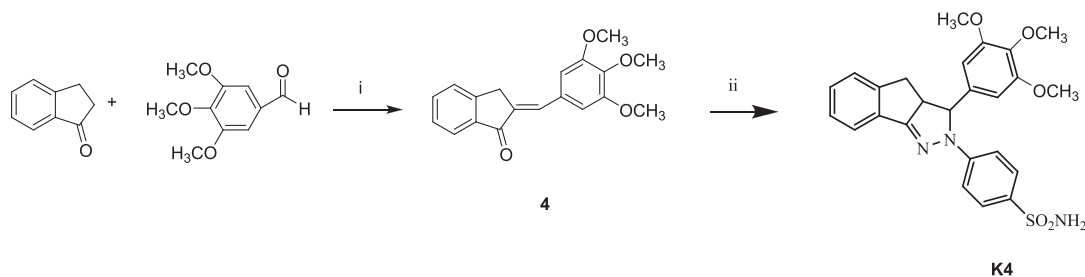
BSA, molar mass ~66 kDa, ethanol (spectrophotometric grade), DMSO (spectrophotometric grade), Trizma (Tris) and HCl (36.5%) were obtained from Sigma.

### 2.2 | Apparatus

<sup>1</sup>H and <sup>13</sup>C nuclear magnetic resonance (NMR) spectra were recorded on Varian 400 and Bruker 400 instruments in DMSO-d<sub>6</sub>. UV-vis light



**SCHEME 1** Molecular structure of **K4**



**SCHEME 2** Synthesis of **K4**

absorption and the fluorescence spectra of the samples were recorded using a Perkin Elmer Lambda 35 UV/VIS spectrophotometer and a Shimadzu RF-5301PC spectrofluorophotometer, respectively.<sup>[17]</sup> For the steady-state fluorescence measurements, sample solutions were excited at 280 nm and fluorescence intensities were recorded between 290 nm and 550 nm. Fluorescence spectra were collected at  $\Delta\lambda = 15$  nm and  $\Delta\lambda = 60$  nm using synchronous fluorescence measurements.<sup>[18]</sup> Fourier transform infrared (FTIR) spectroscopy measurements of the samples were recorded with a Vertex 80/80v FTIR spectrometer.

### 2.3 | Synthesis of **K4**

The compounds were synthesized and characterized as described in our previous study.<sup>[16]</sup> Synthesis of the compounds is summarized in Scheme 2. An aqueous solution of sodium hydroxide (10% w/v, 10 ml) was added into an ethanol (6 ml) solution of 1-indanone (20 mmol) and 3,4,5-trimethoxybenzaldehyde (20 mmol) (Scheme 2). The mixture was stirred overnight at room temperature and then poured onto ice-water (100 ml) in a beaker. The mixture was neutralized with hydrochloric acid (10% w/v, 10 ml). The coloured precipitate formed was filtered and crystallized from the water-ethanol mixture to prepare the chalcone compound, **4** (2-(3,4,5-trimethoxybenzylidene)-2,3-dihydro-1H-inden-1-one). After that, a solution of **4** (1.00 mmol) and 4-hydrazinobenzensulfonamide hydrochloride (1.10 mmol) in ethanol (50 ml) was heated at 100°C, 200 W, 7 bar for 10 min and monitored by thin layer chromatography (TLC). After the reaction was stopped, the volume of the reaction mixture was concentrated to half and the precipitate formed was filtered, washed with cold ethanol, and the compounds were purified by crystallization from ethanol to obtain **K4**. The chemical structure of the compound **K4** was confirmed by <sup>1</sup>H nuclear magnetic resonance (NMR), <sup>13</sup>C NMR, and high resolution mass spectrometry (HRMS). Melting point (M.p.) was 266–269°C.<sup>[16]</sup>

### 2.4 | Preparation of BSA, **K4**, and BSA-**K4** solutions

Tris-HCl buffer solution consisting of 0.2 M Tris was adjusted to pH 7.4 with 36.5% HCl. BSA concentration was kept constant at

10  $\mu\text{M}$  in Tris-HCl buffer solution (pH 7.4). A stock solution of **K4** was prepared in ethanol at  $1.0 \times 10^{-3}$  M. Successive aliquots of **K4** were added (final concentrations of 10; 20; 30; 40; 50; 70; 80 and 100  $\mu\text{M}$ ) using a 100  $\mu\text{l}$  pipette into a vial. The solvent was evaporated using argon gas purging and then the buffer solution containing 10  $\mu\text{M}$  of BSA was added to the vial.<sup>[4]</sup> BSA concentration was kept constant as 10  $\mu\text{M}$  while the fluorescent probe (**K4**) concentration was changed (10–100  $\mu\text{M}$ ) for all studies.

### 3 | RESULTS AND DISCUSSION

#### 3.1 | Fluorescence quenching process of BSA and **K4**

The **K4** compound studied was synthesized as previously described<sup>[16]</sup> and summarized in Scheme 2. Optical properties of **K4** (100  $\mu\text{M}$ ) were determined in Tris-HCl buffer solution (pH 7.4) using UV-vis light absorption and fluorescence measurements (Figure 1). **K4** exhibited two absorption bands at 278 nm and 363 nm and produced a fluorescence band at 465 nm in Tris-HCl buffer solution (pH 7.4). The absorption bands of **K4** at 278 nm and 363 nm corresponded to  $n \rightarrow \pi^*$  transitions and  $\pi \rightarrow \pi^*$  transitions, respectively, of the conjugated skeleton localized on the pyrazoline ring.<sup>[17]</sup>

UV-vis light absorption and fluorescence measurements were also used to determine the optical properties of BSA (10  $\mu\text{M}$ ) in Tris-HCl buffer solution (pH 7.4) (Figure 2). BSA exhibited an absorption band at 275 nm and produced a fluorescence band at 337 nm in Tris-HCl buffer solution (pH 7.4). It is known that the absorption and fluorescence peaks of the BSA molecule are associated with the presence of aromatic amino acids such as tryptophan (Trp), tyrosine (Tyr) and phenylalanine (Phe) in its structure.<sup>[19,20]</sup>

UV-vis light absorption measurements are generally used to understand a ground-state complex formation between a protein and the fluorescent molecule.<sup>[21]</sup> To this aim, the effect of **K4** concentration on the absorption spectra of BSA in Tris-HCl buffer solution

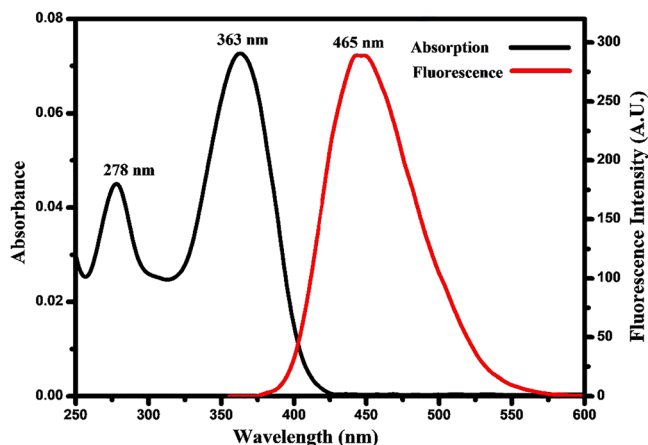


**FIGURE 1** Absorption and fluorescence spectra of **K4** (100  $\mu\text{M}$ ) in Tris-HCl buffer solution (pH 7.4) ( $\lambda_{\text{exc}}$  350 nm)

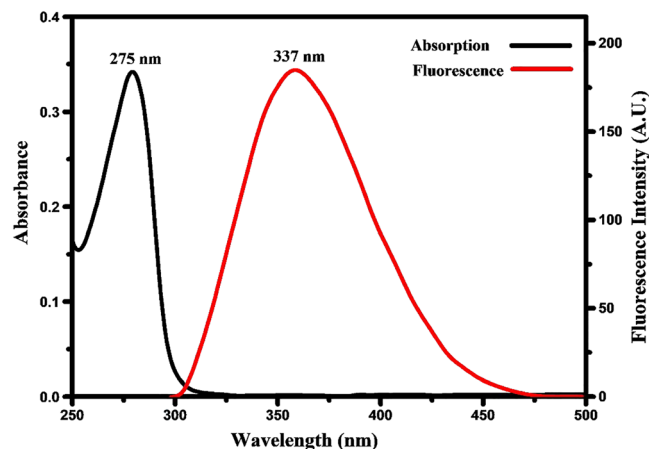


**FIGURE 2** Absorption and fluorescence spectra of BSA (10  $\mu\text{M}$ ) in Tris-HCl buffer solution (pH 7.4) ( $\lambda_{\text{exc}}$  280 nm)

(pH 7.4) was evaluated at room temperature. As can be seen in Figure 3, the absorption band intensity of BSA increased with different concentrations of **K4** and in a concentration-dependent manner due to the interaction between BSA and **K4** in the ground state. BSA itself gave only one absorption peak at 275 nm, but when **K4** was added to the solution, a new absorption band was observed at  $\sim 365$  nm because of the interaction of BSA with **K4**. The peak seen at  $\sim 365$  nm was attributed to the  $\pi \rightarrow \pi^*$  transitions of conjugated skeleton localized on the pyrazoline ring.<sup>[17]</sup> The intensity of the peak at issue increased depending on the **K4** concentration used.

Fluorescence spectroscopy is the most effective and simple method available to understand conformational changes in protein and complex formation between a protein and a probe molecule because of its sensitivity, accuracy, speed, and ease of use at low sample concentrations.<sup>[4,21]</sup> The fluorescence properties of BSA are widely used to investigate binding mechanisms between BSA and drugs. As mentioned previously, BSA contains Trp, Tyr, and Phe aromatic amino acids and the fluorescence properties of BSA come

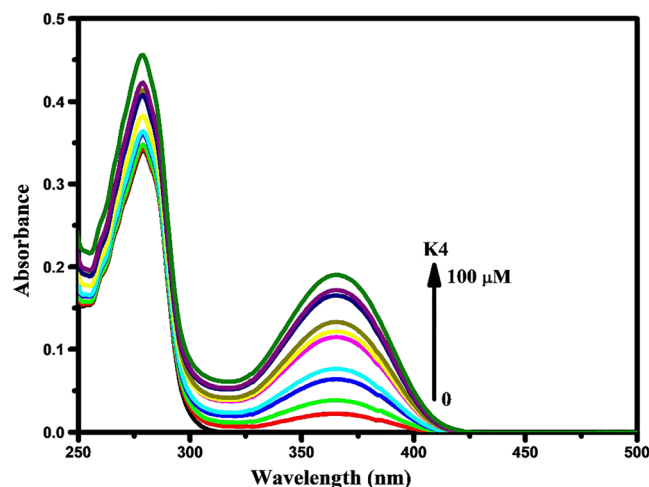


**FIGURE 3** Absorption spectra of BSA with the increasing concentration of **K4** in Tris-HCl buffer solution (pH 7.4)

especially from Trp, as the fluorescence yield of Phe is very low and Tyr has fluorescence quenching properties when ionized.<sup>[22]</sup> When was BSA excited at 280 nm, it exhibited fluorescence because of the available Tyr and Trp residues, but Trp was more dominant in the BSA fluorescence because of the quenching properties of Tyr.<sup>[19]</sup>

Investigation of the BSA fluorescence quenching process using a quencher molecule can reveal the binding mechanism between BSA and quencher. Fluorescence quenching corresponds to a decrease in the fluorescence intensity of a fluorescent probe by the addition of a quencher. The quenching process includes two mechanisms called dynamic and static quenching. If it occurs due to the formation of a nonfluorescent ground-state complex between the fluorophore and the quencher it is called static quenching. In dynamic quenching, diffusive interactions are observed between fluorophore and quencher during the lifetime of the excited state. These two processes are distinguished using temperature, viscosity, or lifetime measurements.<sup>[23]</sup>

Changes in the fluorescence spectra of BSA (10  $\mu\text{M}$ ) dependent on the K4 concentration in buffer solution (pH 7.4) are presented in Figure 4. The fluorescence intensity of BSA decreased gradually and the fluorescence band maxima of BSA displayed a hypsochromic shift ( $\sim 6$  nm) with increasing concentrations of K4. This spectral shift demonstrated the formation of a less polar environment around the Trp and Tyr residues in the BSA structure in the presence of K4.<sup>[24]</sup> In addition, the decrease in fluorescence intensity of BSA was due to the fluorescence quenching process that resulted from the binding between BSA and K4. The mechanism of this fluorescence quenching process can be explained using the following Stern-Volmer equation (eqn (1)):

$$\frac{I_0}{I} = 1 + K_{SV}[Q] \quad (1)$$

where  $I_0$  and  $I$  are fluorescence intensity in the absence or in the presence of quencher, respectively.  $[Q]$  is the quencher

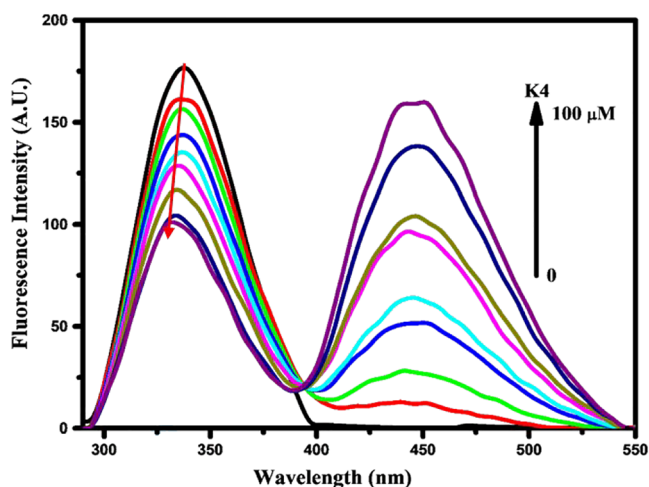


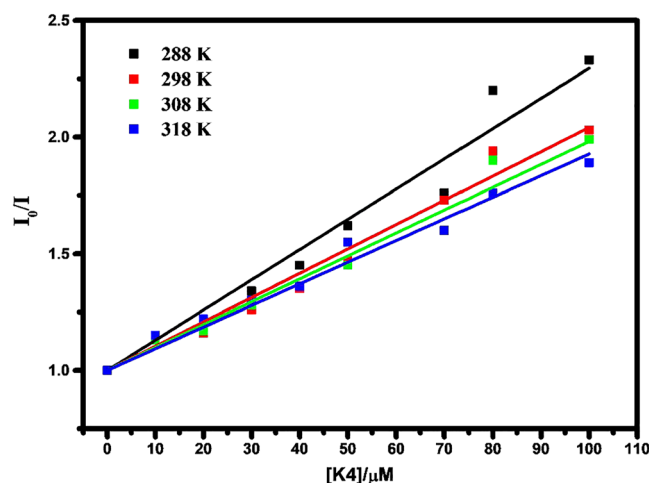
**FIGURE 4** Fluorescence spectra of BSA with the increasing concentration of K4 in Tris-HCl buffer solution (pH 7.4) ( $\lambda_{\text{exc}}$  280 nm)

concentration and  $K_{SV}$  is the Stern-Volmer quenching constant. A Stern-Volmer plot was drawn using the data obtained from fluorescence measurements for the interaction between BSA and K4 at different temperatures (Figure 5). The slope shown in Figure 5 provided the Stern-Volmer quenching constants at various temperatures (Table 1). As shown in Table 1,  $K_{SV}$  values decreased when the temperature was increased. These results indicated that a non-fluorescent complex between the BSA and K4 in the ground state had formed and that the quenching process was due to static quenching.<sup>[21,23,25]</sup>

The binding constant ( $K_b$ ) and the number of binding site ( $n$ ) were determined for the interaction of K4 with BSA using data obtained from fluorescence measurements at four different temperatures.  $K_b$  and  $n$  values were calculated using eqn (2):

$$\log \frac{(I_0 - I)}{I} = \log K_b + n \log [Q] \quad (2)$$

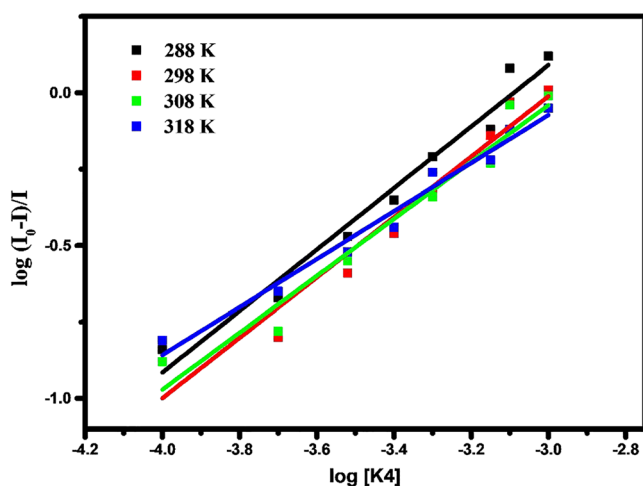
where,  $I$  and  $I_0$  are fluorescence intensity of protein in presence or absence of quencher, respectively.  $[Q]$  is the quencher concentration. The plot of  $\log[(I_0 - I)/I]$  versus  $\log[Q]$  for the interaction of K4 with BSA at four different temperatures are represented in Figure 6. The number of binding sites ( $n$ ) for K4 to BSA was determined from the slope of Figure 6 and  $n$  values are summarized in Table 1. The values in Table 1 reflected that K4 bound to BSA only on one site and that the molecular ratio of the complex between BSA and K4 was 1:1. According to the data,  $K_b$  and  $n$  values decreased when the temperature increased. This suggested that the ground-state complex BSA-K4 forming the binding interaction was unstable. However, the BSA-K4 complex was more stable when tested at low temperatures and, when the temperature increased, the structure of BSA changed. The fact that  $K_b$  values decreased when the temperature increased reflected that the process of quenching between BSA and K4 occurred via a static quenching mechanism.



**FIGURE 5** Stern-Volmer plot for steady-state BSA fluorescence quenching by K4 at 288 K, 298 K, 308 K, and 318 K

**TABLE 1** Stern–Volmer quenching constant and binding parameters for the interaction of BSA with K4 at different temperatures

T (K)	Stern–Volmer quenching constant		Binding parameters		
	$K_{SV} \times 10^5 (M^{-1})$	$r^2$	$n$	$K_b \times 10^3 (M^{-1})$	$r^2$
288	1.35	0.9972	1.01	1.29	0.9655
298	1.04	0.9986	0.99	0.91	0.9444
308	0.98	0.9985	0.93	0.56	0.9508
318	0.93	0.9990	0.78	0.19	0.9716

**FIGURE 6** Double logarithmic plots for fluorescence quenching of BSA (10  $\mu$ M) with different concentrations of K4 in Tris–HCl buffer solution (pH 7.4) at different temperatures

### 3.2 | Determination of interaction forces between BSA–K4 using thermodynamic parameters

It is known that interactions between protein and fluorescent molecule are caused by noncovalent interactions such as van der Waals forces, hydrogen bonding interaction, hydrophobic interaction, and electrostatic interaction. To understand the forces responsible for interactions between protein and fluorophore, it is important to determine thermodynamic parameters such as the enthalpy change ( $\Delta H$ ), entropy change ( $\Delta S$ ), and free energy change ( $\Delta G$ ). The type of possible interaction can be determined by considering the direction of thermodynamic parameters. For this, there are three possibility: (1) if  $\Delta H$  and  $\Delta S$  values are both positive, a hydrophobic interaction is present; (2) if van der Waals forces and/or hydrogen bonding interaction are available,  $\Delta H$  and  $\Delta S$  values are both negative; and (3) if  $\Delta H$  is negative and  $\Delta S$  is positive, electrostatic interactions are present.<sup>[25]</sup> To determine the type of interaction between K4 and BSA, the thermodynamic parameters were calculated using the van 't Hoff equation eqn (3) and the thermodynamic equation eqn (4):

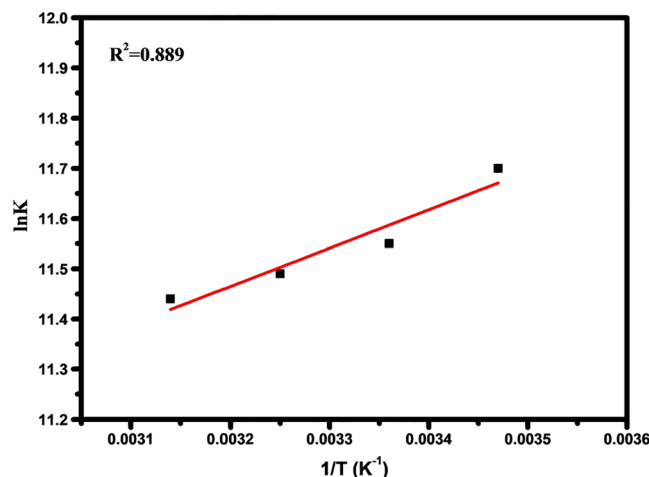
$$\ln K = -\frac{\Delta H}{RT} + \frac{\Delta S}{R} \quad (3)$$

$$\Delta G = \Delta H - T\Delta S \quad (4)$$

where  $K$  is the Stern–Volmer quenching constants,  $R$  is the ideal gas constant and  $T$  is the temperature (K). The plot of  $\ln K$  versus  $1/T$  was drawn using the data obtained from fluorescence measurements at different temperatures (Figure 7).  $\Delta H$  (the slope of plot) and  $\Delta S$  (the intercept of plot) values were calculated from Figure 7. Conversely,  $\Delta G$  values were calculated using eqn (4) obtained with  $\Delta H$  and  $\Delta S$  values. These values are presented in Table 2. The negative  $\Delta G$  values at the studied temperatures indicated that the bonding process was spontaneous. The calculated  $\Delta H$  (negative) and  $\Delta S$  (positive) values from Figure 7 indicated that the main force responsible for the binding interaction of K4 with BSA was electrostatic interaction.

### 3.3 | Energy transfer from BSA to K4

Fluorescence resonance energy transfer (FRET) is used in many fields such as photosensitization, ion sensors, and investigation of supramolecular interactions. FRET is a process in which energy is transmitted from one fluorescence molecule (donor = D) to another molecule (acceptor = A). The transfer from donor molecule to acceptor molecule takes place nonradiatively. The possibility of energy transfer depends on parameters such as quantum yield of the donor, spectral overlap between the donor emission and the acceptor absorption spectra, relative orientation of the donor and acceptor transition dipoles, and the distance between donor and acceptor transition dipoles.<sup>[26]</sup>

**FIGURE 7** van 't Hoff plot for the interaction of K4 with BSA

**TABLE 2** Thermodynamic parameters for the interaction of BSA with K4 at different temperatures

T (K)	$\Delta G$ (kJmol <sup>-1</sup> )	$\Delta H$ (kJmol <sup>-1</sup> )	$\Delta S$ (jmol <sup>-1</sup> K <sup>-1</sup> )
288	-27.95	-6.35	75.00
298	-28.70		
308	-29.45		
318	-30.20		

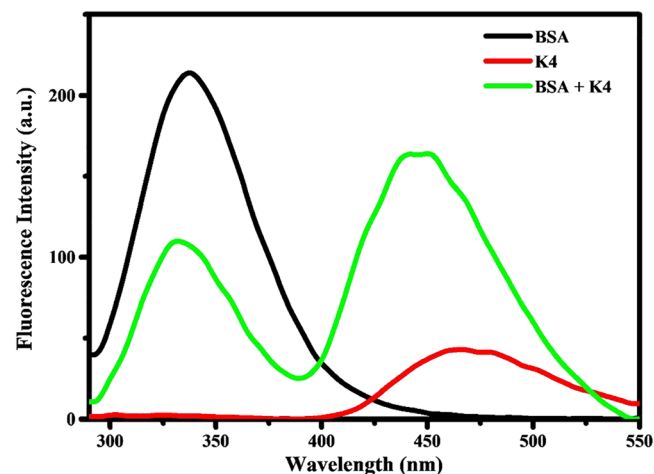
The fluorescence measurements for BSA, K4 and the BSA-K4 pair were taken at the excitation wavelength of the donor ( $\lambda_{exc} = 280$  nm), to show that there may be energy transfer between BSA and K4. The fluorescence spectrum of BSA-K4 pair gave two peaks at 331 and 445 nm (Figure 8). As can be seen in Figure 8, the fluorescence peak of the BSA-K4 pair at 331 nm had a lower intensity than the peak from BSA alone; the fluorescence peak of the BSA-K4 pair at 445 nm had higher intensity than the peak which belonged to K4 alone. This result proved the possibility of energy transfer between BSA and K4.<sup>[26]</sup>

The energy transfer efficiency (E) is one of the important parameters for FRET. E was calculated using equation below (eqn (5))<sup>[23]</sup>:

$$E = 1 - \frac{I_{DA}}{I_D} = \frac{R_0^6}{R_0^6 + r_0^6} \quad (5)$$

where  $I_D$  is the relative fluorescence intensity of the donor in the absence of acceptor and  $I_{DA}$  is the relative fluorescence intensity of the donor in the presence of acceptor,  $r_0$  is the distance between donor and acceptor and  $R_0$  is a distance at which energy transfer efficiency is 50%. This distance can be calculated using the following equation (eqn (6)):

$$R_0 = 0.211 [\kappa^2 \eta^{-4} Q_D J(\lambda)]^{1/6} \quad (6)$$

**FIGURE 8** Fluorescence spectra of BSA (10 μM), K4 (100 μM) and BSA-K4 in Tris-HCl buffer solution (pH 7.4) ( $\lambda_{exc}$  280 nm)

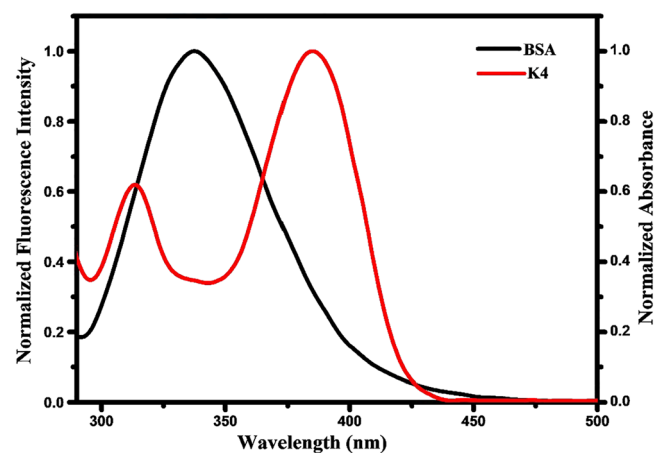
where  $Q_D$  is the quantum yield of the donor in the absence of the acceptor,  $\eta$  is the refractive index of the medium,  $\kappa^2$  (2/3) is the orientation factor<sup>[26]</sup>  $\eta$  and  $Q_D$  were used as 1.3361 and 0.15, respectively in this study.<sup>[27]</sup>  $J(\lambda)$  is the spectral overlap integral between the emission spectrum of the donor and the absorption spectrum of acceptor and this value was calculated using eqn (7):

$$J(\lambda) = \frac{\int_0^\infty F_D(\lambda) \epsilon_A(\lambda) \lambda^4 d\lambda}{\int_0^\infty F_D(\lambda) d\lambda} \quad (7)$$

where  $F_D(\lambda)$  is the normalized fluorescence intensity of the donor in the absence of acceptor and  $\epsilon_A(\lambda)$  is the extinction coefficient of the acceptor. The spectral overlap for BSA and K4 is presented in Figure 9.  $J(\lambda)$  was calculated as  $6.47 \times 10^{12}$  using eqn (7). Moreover, the values of E,  $R_0$  and  $r_0$  were 50.0%, 1.62 nm and 1.64 nm, respectively. The indication of high probability energy transfer between the donor (BSA) and the acceptor (K4) is that the distance between the donor-acceptor is on the 2–8 nm scale with the rule  $0.5R_0 < r_0 < 1.5R_0$ .<sup>[28]</sup>

### 3.4 | Investigation of changes in BSA conformation with K4 binding

Synchronous fluorescence is one technique used to examine changes in the conformation of a protein. BSA has fluorescence properties due to the presence of the Trp, Tyr, and Phe residues. The polarity changes around the Tyr or Trp residues are analyzed using  $\Delta\lambda$  (the difference between the excitation wavelength and the emission wavelength) values. If  $\Delta\lambda$  is 15 nm, the synchronous fluorescence spectrum of BSA reflects changes around the Tyr residue. However, if  $\Delta\lambda = 60$  nm, the synchronous fluorescence spectrum of BSA reflects the changes around the Trp residue.<sup>[29]</sup> The changes in the BSA synchronous fluorescence spectra with increasing K4 concentration are given in Figure 10(a, b). When  $\Delta\lambda$  was 60 nm, the fluorescence intensity of the Trp residue of BSA decreased regularly and the

**FIGURE 9** Spectral overlap between BSA and K4

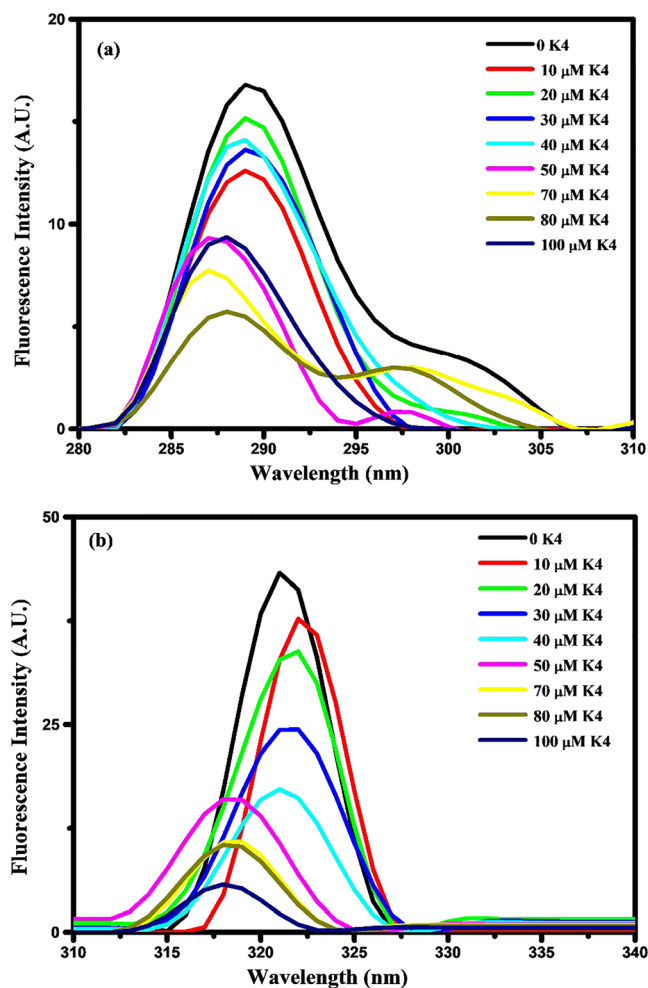


**FIGURE 10** Synchronous fluorescence spectra of BSA (10  $\mu\text{M}$ ) at pH 7.4 in the presence of different concentration of K4 at room temperature  $\Delta\lambda$  15 nm (a) and  $\Delta\lambda$  60 nm (b)

fluorescence peak maxima of BSA were significantly blue shifted (from 321 nm to 317 nm) with addition of K4. When  $\Delta\lambda$  is 15 nm, the fluorescence intensity of the Tyr residue of BSA did not change regularly with K4 concentration. These results suggested that the conformation of the Trp residue was more affected than Tyr upon BSA–K4 interaction.<sup>[30]</sup>

To investigate possible perturbations in the BSA structure upon addition of a K4 solution, we performed some experiments using FTIR spectroscopy. The amide I and amide II bands of proteins in the 1600–1700 and 1500–1600  $\text{cm}^{-1}$  region, respectively, provided useful information about protein conformation in the native and unfolded states. Figure 11 shows the FTIR spectra of BSA in the absence or presence of K4. In the absence of K4, the infrared spectrum for BSA presented two peaks at 1648 and 1555  $\text{cm}^{-1}$  assigned to amide I and amide II, respectively. When the FTIR spectrum was recorded in the presence of K4, the amide I and amide II bands remained unchanged, not only in their relative position, but also in relative intensity. These results showed that there was no significant change in the polarity around the Trp residue.<sup>[21]</sup>

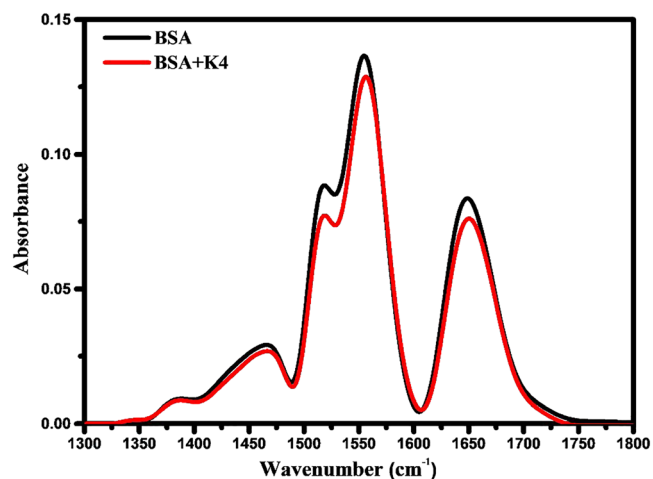


**FIGURE 11** FTIR spectrum of BSA (10  $\mu\text{M}$ ) in the absence or presence of K4 (100  $\mu\text{M}$ )

## 4 | CONCLUSION

This study focused on the interaction between BSA and K4, which is a new pyrazoline derivative, using UV–vis light absorption, and steady-state and synchronous fluorescence measurements. The results showed that static quenching occurred between K4 and BSA by means of ground-state complex formation. This result was confirmed by determining that the Stern–Volmer quenching constant decreased with increasing temperature. The binding constant and binding site values calculated at four different temperatures reflected that BSA and K4 formed a complex in a 1:1 molecular ratio and that their binding interactions were not stable. It was determined that the binding process was spontaneous and the BSA–K4 interaction was electrostatic according to the thermodynamic parameters calculated using the van 't Hoff equation. Energy transfer between BSA–K4 was also examined. It was observed that there was a high rate of energy transfer (50.0%) between two molecules. The changes in the conformation of BSA via binding of K4 were discussed with synchronous fluorescence measurements. The results revealed that K4 bound to the BSA molecule from the Trp region. FTIR measurements were recorded to investigate possible perturbations in the BSA structure upon addition of a K4 solution. FTIR results showed that there was no significant change in the polarity around the Trp residue. It is thought that the determination of interactions between the possible drug candidate compound K4 and the model protein BSA will provide very useful information for researchers for biophysical studies.

## ACKNOWLEDGEMENTS

Authors thank Mehtap Tugrak for her kind contributions during the synthesis and NMR studies of this compound.

## ORCID

Ebru Bozkurt  <https://orcid.org/0000-0002-5345-9718>

## REFERENCES

- [1] T. Bayraktutan, Y. Onganer, *Spectrochim. Acta, Part A* **2017**, *171*, 90.
- [2] K. Ghosh, S. Rathi, D. Arora, *J. Lumin.* **2016**, *175*, 135.
- [3] B. K. Paul, N. Guchhait, S. C. Bhattacharya, *J. Photochem. Photobiol., B* **2017**, *172*, 11.
- [4] O. A. Chaves, V. A. da Silva, C. M. R. Sant'Anna, A. B. B. Ferreira, T. A. N. Ribeiro, M. G. de Carvalho, D. Cesarin-Sobrinho, J. C. Netto-Ferreira, *J. Mol. Struct.* **2017**, *1128*, 606.
- [5] P. Banerjee, S. Pramanik, A. Sarkar, S. C. Bhattacharya, *J. Phys. Chem. B* **2009**, *113*(33), 11429.
- [6] A. Salci, M. Toprak, *J. Biomol. Struct. Dyn.* **2017**, *35*(1), 8.
- [7] M. Toprak, *Spectrochim. Acta, Part A* **2016**, *154*, 108.
- [8] N. C. Desai, D. Pandya, D. Vaja, *Med. Chem. Res.* **2018**, *27*(1), 52.
- [9] Z. A. Kaplancikli, G. Turan-Zitouni, A. Özdemir, Ö. Devrim Can, P. Chevallet, *Eur. J. Med. Chem.* **2009**, *44*(6), 2606.
- [10] P. Ravula, H. B. Vamaraju, M. Paturi, S. Bodige, K. C. Gulipalli, J. N. N. S. Chandra, *J. Heterocyclic Chem.* **2018**, *55*(6), 1313.
- [11] H. I. Gul, C. Yamali, F. Yesilyurt, H. Sakagami, K. Kucukoglu, I. Gulcin, M. Gul, C. T. Supuran, *J. Enzyme Inhib. Med. Chem.* **2017**, *32*(1), 369.
- [12] A. Özdemir, M. Altintop, Z. Kaplancikli, Ö. Can, Ü. Demir Özkay, G. Turan-Zitouni, *Molecules* **2015**, *20*(2), 2668.
- [13] S. N. Shringare, H. V. Chavan, P. S. Bhale, S. B. Dongare, Y. B. Mule, S. B. Patil, B. P. Bandgar, *Med. Chem. Res.* **2018**, *27*(4), 1226.
- [14] A. Sarkar, S. C. Bhattacharya, *J. Lumin.* **2012**, *132*(10), 2612.
- [15] A. Burmudžija, Z. Ratković, J. Muškinja, N. Janković, B. Ranković, M. Kosanić, S. Đorđević, *RSC Adv.* **2016**, *6*(94), 91420.
- [16] H. I. Gul, M. Tugrak, H. Sakagami, P. Taslimi, I. Gulcin, C. T. Supuran, *J. Enzyme Inhib. Med. Chem.* **2016**, *31*(6), 1619.
- [17] E. Bozkurt, H. I. Gul, E. Mete, *J. Photochem. Photobiol., A* **2018**, *352*, 35.
- [18] J. Guan, X. Yan, Y. Zhao, Y. Sun, X. Peng, *Spectrochim. Acta, Part A* **2018**, *202*, 1.
- [19] M. S. Ali, H. A. Al-Lohedan, *J. Mol. Liq.* **2017**, *236*, 232.
- [20] J. Gao, Y. Guo, J. Wang, Z. Wang, X. Jin, C. Cheng, Y. Li, K. Li, *Spectrochim. Acta, Part A* **2011**, *78*(4), 1278.
- [21] O. A. Chaves, D. Cesarin-Sobrinho, C. M. R. Sant'Anna, M. G. de Carvalho, L. R. Suzart, F. E. A. Catunda-Junior, J. C. Netto-Ferreira, A. B. B. Ferreira, *J. Photochem. Photobiol., A* **2017**, *336*, 32.
- [22] H. Mohammadzadeh-Aghdash, J. Ezzati Nazhad, P. D. Dolatabadi, V. Panahi-Azar, A. Barzegar, *Food Chem.* **2017**, *228*, 265.
- [23] J. R. Lakowicz, *Principles of fluorescence spectroscopy*, Springer Science & Business Media, New York **2013**.
- [24] J. A. Molina-Bolívar, C. C. Ruiz, F. Galisteo-González, M. M. O'Donnell, A. Parra, *Fluid Phase Equil.* **2015**, *400*, 43.
- [25] J.-h. Shi, D.-q. Pan, X.-x. Wang, T.-T. Liu, M. Jiang, Q. Wang, *J. Photochem. Photobiol., B* **2016**, *162*, 14.
- [26] E. Bozkurt, Y. Onganer, *Synth. Met.* **2018**, *245*, 260.
- [27] J. Gao, Z. Wang, J. Wang, X. Jin, Y. Guo, K. Li, Y. Li, P. Kang, *Spectrochim. Acta, Part A* **2011**, *79*(5), 849.
- [28] Z. Bai, Y. Liu, P. Zhang, J. Guo, Y. Ma, X. Yun, X. Zhao, R. Zhong, F. Zhang, *Luminescence* **2016**, *31*(3), 688.
- [29] M. Makarska-Bialokoz, *Spectrochim. Acta, Part A* **2018**, *193*, 23.
- [30] B. Aneja, M. Kumari, A. Azam, A. Kumar, M. Abid, R. Patel, *Luminescence* **2018**, *33*(3), 464.

**How to cite this article:** Bozkurt E, Gul HI. Deciphering binding mechanism between bovine serum albumin and new pyrazoline compound K4. *Luminescence*. 2019;1–8. <https://doi.org/10.1002/bio.3762>